

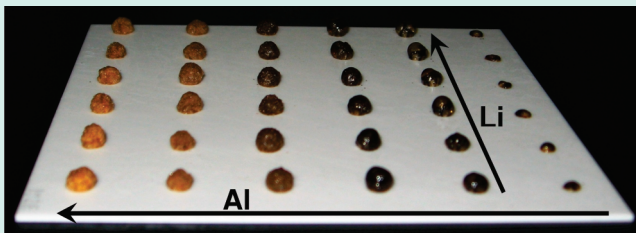
Combinatorial Synthesis of Mixed Transition Metal Oxides for Lithium-Ion Batteries

Graham H. Carey^{†,‡} and J. R. Dahn^{*,†,‡}

[†]Department of Chemistry and [‡]Department of Physics and Atmospheric Science, Dalhousie University, Halifax, Nova Scotia B3H 3J5, Canada

 Supporting Information

ABSTRACT: Many methods exist for the synthesis of lithium metal oxides for use as positive electrode materials in lithium-ion batteries; however, no such method to date is both combinatorial (able to process broad ranges of compositional space quickly and efficiently) and well-studied to ensure confidence in the procedure. This study develops a procedure for microliter-scale solution-processing synthesis using a combinatorial solution-processing robot. Two compositional systems ($\text{LiNi}_{x}\text{Mn}_{2-x}\text{O}_4$ and Li-Al-Mn oxide) were synthesized to compare the method to existing syntheses to ensure confidence in the procedure. Samples produced by this new synthetic procedure have crystal structures and lattice constants that closely match those of bulk-prepared samples found in the literature.



samples produced by this new synthetic procedure have crystal structures and lattice constants that closely match those of bulk-prepared samples found in the literature.

KEYWORDS: mixed transition metal oxides, lithium-ion batteries, microliter-scale, solution-processing robot, combinatorial libraries

INTRODUCTION

Lithium-ion batteries remain at the forefront of next-generation energy storage research. Re-examinations of existing materials and increased exploration of unexamined material compositional space are ever more important with the advent of commercially available electric vehicles that need increased energy density batteries. Positive electrode materials, especially lithium mixed-metal oxides, present a unique challenge to materials researchers to ensure that the metal cations are uniformly mixed at an atomic level. To date, bulk synthetic methods, such as solid-state synthesis,¹ solution coprecipitation,² or sol-gel preparation³ have been used to make materials like $\text{LiNi}_{0.5}\text{Mn}_{1.5}\text{O}_4$ (solid state) and $\text{Li}[\text{Ni}_{1/3}\text{-Mn}_{1/3}\text{-Co}_{1/3}]_{\text{O}_2}$ (coprecipitation). These methods, while useful for synthesizing large amounts of consistent single-composition material, are expensive and time-consuming when applied over a broader range of compositional space, with the one-composition-at-a-time approach consuming large amounts of resources to produce material of initially uncertain usefulness.

A combinatorial approach is much more efficient for synthesizing broad ranges of compositional space for subsequent analysis of physical and electrochemical properties. Physical vapor deposition techniques (such as sputtering) used successfully in the combinatorial synthesis of negative electrode materials⁴ employ conditions not ideally suited to the creation of lithium mixed-metal oxides. Some work has been done using combinatorial milling,⁵ followed by heat-treatment, however while this method reduces the time required to synthesize broad composition ranges of samples, there was no proof that metal atom mixing at the atomic scale was achieved. A more suitable technique involves a scaled-down application of bulk solution-based syntheses, using varying amounts of precursor solutions to create small samples

across a broad range of compositions in a timely, efficient manner. An analogous technique, using a solutions-processing robot to ensure accurate, small volume dispenses, has been utilized elsewhere in materials research in the synthesis of ceramics.^{5,6}

This study focuses on the development and confidence-testing of a solutions-processing robot method applied to positive electrode materials for lithium-ion batteries. While similar surveys have been performed recently,⁷⁻⁹ no studies take full account of factors, such as heating conditions, substrate choice, or a comparison of synthesized sample lattice constants to accepted literature values. This study tests the developed procedure on two positive electrode material systems; a linear $\text{LiNi}_{x}\text{Mn}_{2-x}\text{O}_4$ system and a ternary Li-Al-Mn spinel oxide system. The final procedure should allow for confident future explorations of positive electrode material compositional space.

RESULTS AND DISCUSSION

Synthetic Method. All samples were prepared by microliter-scale solution deposition using a Cartesian Pixsys solution-processing robot. Solutions were deposited on stearic acid-coated alumina plates, using coprecipitation or a viscous sucrose solution additive to maintain even dispersal of the metal cations until heat treatment. Samples were preheated at low temperature to drive off water, then heat treated in air at temperatures ranging from 500 to 900 °C to produce the desired lithium metal oxides. Figure 1 shows a typical Li-Al-Mn spinel system sample before heat treatment, with Al and Li increasing as indicated.

Received: November 9, 2010

Revised: November 26, 2010

Published: January 06, 2011

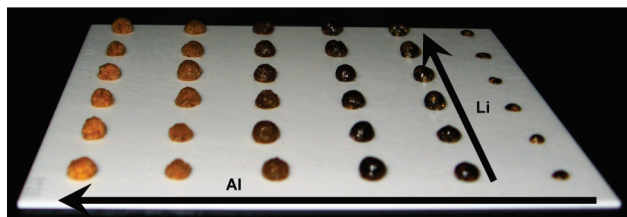


Figure 1. Li–Al–Mn salt/sucrose mixtures after heating at 55 °C for 24 h, with aluminum and lithium amounts increasing as indicated.

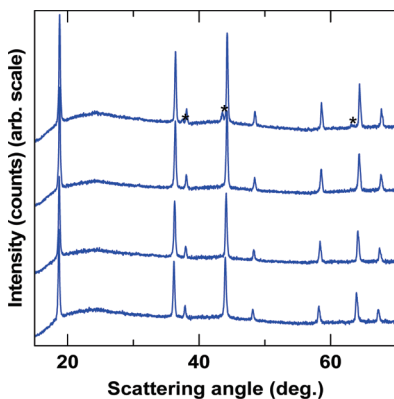


Figure 2. Powder X-ray diffraction patterns for $\text{LiNi}_x\text{Mn}_{2-x}\text{O}_4$ with decreasing x from top to bottom, prepared by carbonate coprecipitation at 800 °C. Peaks marked * are rock-salt impurities ($\text{Li}_x\text{Ni}_{1-x}\text{O}$) that appear at high nickel content.

Structural Characterization. The crystallographic structure of the samples was assessed with a Bruker D8 Discover X-ray system equipped with an xyz translation stage, a Cu target X-ray tube, an incident beam monochromator to select Cu $\text{K}\alpha$ radiation and an area detector placed 20.0 cm from the center of the measurement circle. A laser and video system was used to align each individual library position to the center of the measurement circle. Samples were held stationary during measurement since the surfaces of the powder “dots” were not perfectly flat. The incident beam was collimated to a diameter of 0.5 mm. The detector was set to sample three frames per compositional spot, for a total scattering angle range between 15 and 70°. XRD spectra were collected for each compositional point, counting for 300 s for each frame. Lattice constants were calculated by fitting pseudo-Voigt peaks to the data, using a combination of readily available freeware (gnuplot and Irfanview) and in-house developed software.

XRD Characterization of $\text{LiNi}_x\text{Mn}_{2-x}\text{O}_4$ System. Figure 2 shows the powder diffraction patterns for selected members of the $\text{LiNi}_x\text{Mn}_{2-x}\text{O}_4$ system prepared at 800 °C. Pictured, from top to bottom, are $\text{LiNi}_{0.5}\text{Mn}_{1.5}\text{O}_4$, $\text{LiNi}_{0.375}\text{Mn}_{1.625}\text{O}_4$, $\text{LiNi}_{0.25}\text{Mn}_{1.75}\text{O}_4$, and $\text{LiNi}_{0.125}\text{Mn}_{1.875}\text{O}_4$. As expected from literature,¹⁰ the rock-salt phase $\text{Li}_x\text{Ni}_{1-x}\text{O}$ appears at high nickel content, as indicated by the stars in the figure. Otherwise, no impurities are present, and the procedure leads to clear, well-defined peaks characteristic of well-mixed, single-phase samples.

Figure 3 shows the full set of powder diffraction patterns for the sample discussed above, with x increasing from 0.025 to 0.5 in steps of 0.025 from bottom to top, with the pattern zoomed in on the 311, 222, and 400 peaks to emphasize the shift in peak position with increasing nickel content, x . As expected,¹¹ as the

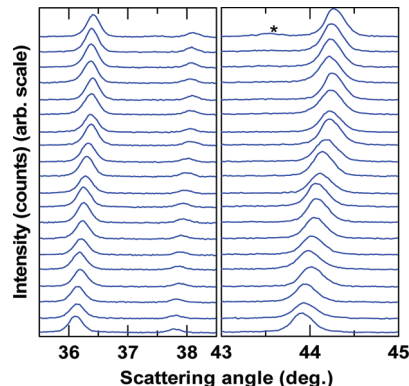


Figure 3. Bragg peak shifts near 36, 38, and 44 degrees for $\text{LiNi}_x\text{Mn}_{2-x}\text{O}_4$ samples prepared by carbonate coprecipitation at 800 °C, with decreasing x top to bottom. Peaks marked * are rock-salt impurities ($\text{Li}_x\text{Ni}_{1-x}\text{O}$) that appear at high nickel content.

Table 1. Measured and Calculated Bragg Peak Positions for a Representative $\text{LiNi}_x\text{Mn}_{2-x}\text{O}_4$ Sample, Corrected for an Off-Axis Displacement of $-19.2\ \mu\text{m}$ by In-House Developed Least-Squares Fitting Software^a

| <i>hkl</i> | observed angle (deg) | corrected angle (deg) | calculated angle (deg) | difference |
|------------|-------------------------|--------------------------|---------------------------|------------|
| 111 | 18.674 | 18.686 | 18.677 | 0.009 |
| 311 | 36.183 | 36.195 | 36.205 | -0.01 |
| 222 | 37.862 | 37.874 | 37.875 | -0.001 |
| 400 | 44.005 | 44.016 | 44.017 | 0 |
| 331 | 48.188 | 48.199 | 48.204 | -0.005 |
| 511 | 58.259 | 58.27 | 58.261 | 0.009 |
| 440 | 63.997 | 64.007 | 64.006 | 0.001 |
| 531 | 67.307 | 67.317 | 67.318 | -0.001 |

^a The calculated angles are those based on the best-fit cubic lattice constant.

nickel ions replace the larger manganese ions in the crystal lattice, the lattice size shrinks, leading to peaks shifted further to the right. The shift levels out at high nickel content, likely because of the formation of the rock salt impurity mentioned above. Table 1 shows a representative set of Bragg peak positions for one sample spot of the library, processed by in-house least-squares fitting software to calculate an off-axis displacement correction, with a comparison to a set of peak positions calculated for the most appropriate value of the lattice parameter, a . The agreement between measured and calculated peak positions is excellent.

Figure 4 first shows an overlay of literature data for the composition range synthesized, showing the spread of lattice parameter, a , depending on the synthetic method applied. From the work of Zhong et al.,¹² three data sets are overlaid in Figure 4, including a solid-state preparation at 750 °C and two sol–gel preparations at 600 and 850 °C. Below, the lattice constants extracted from the set of diffraction patterns shown in Figure 3 are plotted in comparison with a representative set of Zhong's data. The experimental data from this work follows the trend observed in other syntheses very well. There is some fluctuation in the data compared to other works, but this falls well within the acceptable spread of lattice parameters as indicated in the top portion of the figure.

XRD Characterization of the Li–Al–Mn Ternary System. Figure 5 shows a representative set of data from the Li–Al–Mn

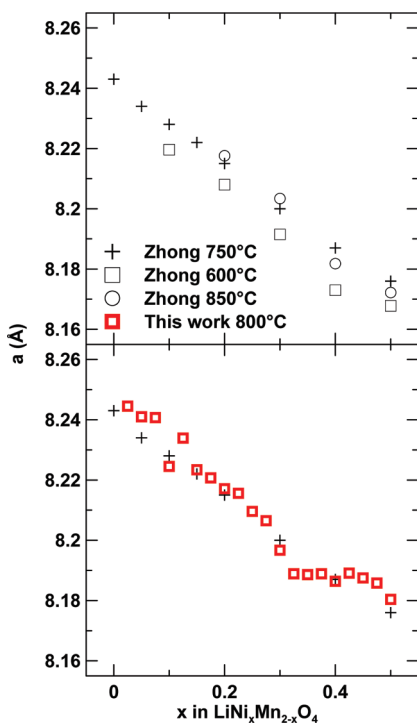


Figure 4. (Top) Solid state (750 °C) and sol–gel (600 and 850 °C) results for the lattice constant, a , versus x in $\text{LiNi}_x\text{Mn}_{2-x}\text{O}_4$ from Zhong et al.¹⁶ (Bottom) Comparison of the lattice constants of $\text{LiNi}_x\text{Mn}_{2-x}\text{O}_4$ prepared by carbonate coprecipitation at 800 °C (this work) to representative data from Zhong.

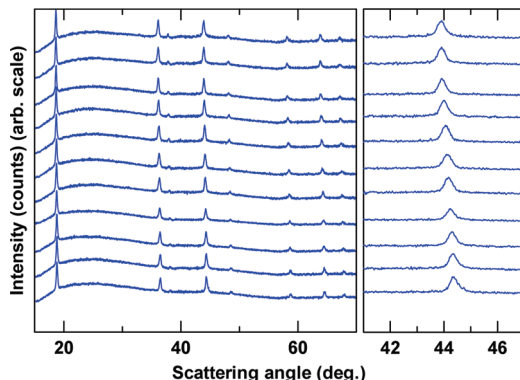


Figure 5. Powder X-ray diffraction patterns for $\text{Li}_{1+x}\text{Mn}_{2-x}\text{O}_4$ with increasing x from top to bottom, prepared by the sucrose matrix method at 700 °C, across the entire scattering angle range (left) and zoomed in on the 400 peak (right).

ternary system, for a set of libraries prepared at 700 °C. The compositional line selected has no Al present and a linear progression from LiMn_2O_4 to $\text{Li}[\text{Li}_{1/3}\text{Mn}_{5/3}]\text{O}_4$ from top to bottom in the figure. The left side of the figure shows the entire scanning range, from 15 to 70°, demonstrating the pure, single phase nature of the generated samples, while the right side is zoomed in near the 400 peak, demonstrating the smooth shift to the right that accompanies a progression to a smaller lattice constant.

Figure 6 shows a contour plot of the lattice constant, a , plotted against fractional composition of LiMn_2O_4 , LiAlMnO_4 and $\text{Li}[\text{Li}_{1/3}\text{Mn}_{5/3}]\text{O}_4$ for the library set prepared at 700 °C. Almost

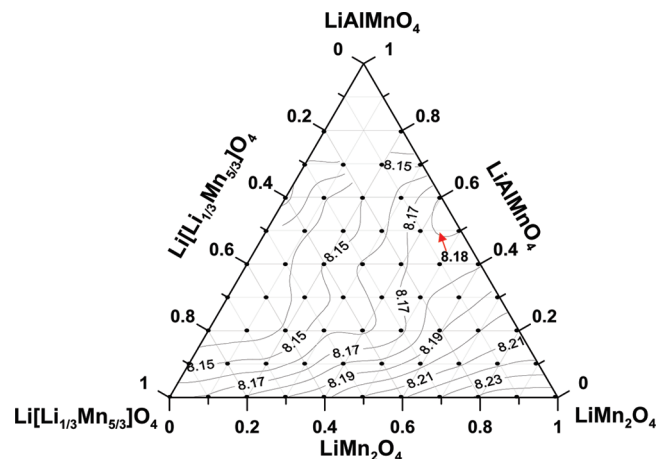


Figure 6. Contour map of the lattice parameter, a , for a combinatorial mixture of LiMn_2O_4 , LiAlMnO_4 , and $\text{Li}[\text{Li}_{1/3}\text{Mn}_{5/3}]\text{O}_4$ prepared by the sucrose matrix method at 700 °C (this work). Dots indicate single-phase spinel-structure samples.

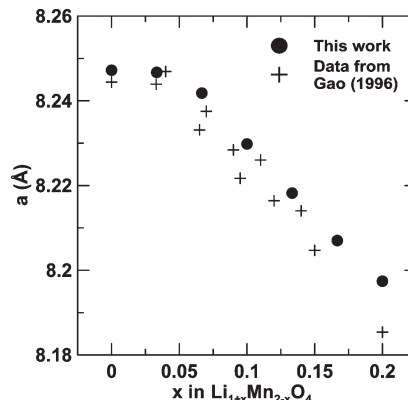


Figure 7. Comparison of Li–Al–Mn oxide spinel lattice constants for samples prepared at 700 °C, along the $\text{Li}_{1+x}\text{Mn}_{2-x}\text{O}_4$ line (this work), to literature values (Gao¹³).

the entire range is single-phase, except the corner representing the highest Al content, where LiAlO_2 impurities show up. Multiphase data has been omitted from the figure.

While this ternary system has not been examined in its entirety in the literature, it is possible to compare portions of the overall data set to accepted results from other authors. Figure 7 examines the lattice constants extracted from the $\text{Li}_{1+x}\text{Mn}_{2-x}\text{O}_4$ composition line in Figure 6, which runs horizontally along the bottom of the diagram. Values from this work are overlaid with lattice constants from Gao's solid state compositions produced at 750 °C.¹³ A slight manganese excess is suspected in the samples produced during this study, which accounts for the slightly larger lattice constants compared to the Gao data, otherwise the robot-generated samples follow the literature trend closely, including the difficulty synthesizing pure LiMn_2O_4 , which accounts for the suppression in lattice constant value at $x = 0$ in both this work and the literature.¹⁴

Figure 8 compares lattice constants extracted from the LiAlMnO_4 compositional line, found to the far right of the plot in Figure 6. The lattice constant drops sharply between $y = 0$ and 0.1, as observed in Xiao's sol–gel compositions annealed at 800 °C.¹⁵ The data then follows a smooth decreasing trend with

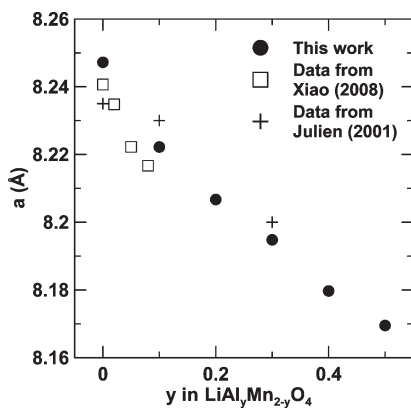


Figure 8. Comparison of Li-Al-Mn oxide spinel lattice constants for samples prepared at 700 °C, along the $\text{LiAl}_y\text{Mn}_{2-y}\text{O}_4$ line (this work), to literature values (Julien¹⁶ and Xiao¹⁵).

increasing Al content, as observed in Julien's sol-gel compositions annealed at 550 °C.¹⁶ As a final comparison of samples generated by this study's procedure to existing data, the point at $\text{Li}[\text{Li}_{0.1}\text{Al}_{0.1}\text{Mn}_{1.8}]\text{O}_4$ has been compared to work by Ohzuku, whose samples were prepared by oxidative solution processing and annealed at 650 °C.¹⁷ The lattice constant of that material was found to be 8.211 Å, compared to a value of 8.1969 Å extracted from the sample generated by this work.

■ CONCLUSION

A combinatorial synthetic procedure was designed and improved using a solution-processing robot to perform small-scale solution mixing across broad ranges of compositional space. Two compositional systems ($\text{LiNi}_x\text{Mn}_{2-x}\text{O}_4$ and Li-Al-Mn spinel oxide) were synthesized to compare the method to existing syntheses to ensure confidence in the procedure. Samples produced by this new synthetic procedure have crystal structures and lattice constants that closely match those of bulk-prepared samples found in the literature.

■ ASSOCIATED CONTENT

5 Supporting Information. Detailed description of the synthetic method, including substrate selection, dispense procedures and heat treatment. This material is available free of charge via the Internet at <http://pubs.acs.org>.

■ AUTHOR INFORMATION

Corresponding Author

*E-mail: jeff.dahn@dal.ca. Phone: 902-494-2991. Fax: 902-494-5191.

■ REFERENCES

- (1) Guyomard, D.; Verbaere, A.; Piffard, Y.; Tournoux, M.; Sigala, C. Positive electrode materials with high operating voltage for lithium batteries: $\text{LiCr}_y\text{Mn}_{2-y}\text{O}_4$ ($0 \leq y \leq 1$). *Solid State Ionics* **1995**, *81*, 167–170.
- (2) Caurant, D.; Baffier, N.; Garcia, B.; Pereira-Ramos, J. P. Synthesis by a soft chemistry route and characterization of $\text{LiNi}_x\text{Co}_{1-x}\text{O}_2$ ($0 \leq x \leq 1$) cathode materials. *Solid State Ionics* **1996**, *91*, 45–54.
- (3) Zheng, T.; Thomas, C. L.; Dahn, J. R. Structure and electrochemistry of $\text{Li}_2\text{Cr}_x\text{Mn}_{2-x}\text{O}_4$ for $1.0 \leq x \leq 1.5$. *J. Electrochem. Soc.* **1998**, *145*, 851–859.

(4) Mar, R. E.; Abouzeid, A.; Dahn, J. R. Combinatorial study of $\text{Sn}_{1-x}\text{Co}_x$ ($0 < x < 0.6$) and $[\text{Sn}_{0.55}\text{Co}_{0.45}]_{(1-y)}\text{C}_y$ ($0 < y < 0.5$) alloy negative electrode materials for Li-ion batteries. *J. Electrochem. Soc.* **2006**, *153*, A361–A365.

(5) Downs, R. High-throughput mechanical alloying and screening. U.S. Patent Appl. 20080085221, April 10, 2008.

(6) Wang, J.; Evans, J. R. G. London University Search Instrument: A combinatorial robot for high-throughput methods in ceramic science. *J. Comb. Chem.* **2005**, *7*, 665–672.

(7) Ohtaki, T.; Watanabe, M.; Yanase, I. Application of combinatorial process to $\text{LiCo}_{1-x}\text{Mn}_x\text{O}_2$ ($0 \leq x \leq 0.2$) powder synthesis. *Solid State Ionics* **2002**, *151*, 189–196.

(8) Ohtaki, T.; Watanabe, M.; Yanase, I. Combinatorial study for ceramics powder by X-ray diffraction. *Solid State Ionics* **2002**, *154*, 419–424.

(9) Takada, K.; Sasaki, T.; Watanabe, M.; Fujimoto, K. Combinatorial approach for powder preparation of pseudo-ternary system $\text{LiO}_{0.5-x}\text{TiO}_2$ ($X = \text{FeO}_{1.5}$, $\text{CrO}_{1.5}$, and NiO). *Appl. Surf. Sci.* **2004**, *223*, 49–53.

(10) Spong, A. D.; Vitins, G.; Owen, J. R. A solution-precursor synthesis of carbon-coated LiFePO_4 for Li-ion cells. *J. Electrochem. Soc.* **2005**, *152*, A2376–A2382.

(11) Tian, L.; Xu, W. M.; Wang, Y. Q.; Yuan, A. B. Al-doped spinel $\text{LiAl}_{0.1}\text{Mn}_{1.9}\text{O}_4$ with improved high-rate cyclability in aqueous electrolyte. *J. Power Sources* **2010**, *195*, 5032–5038.

(12) Zhong, Q.; Bonakdarpour, A.; Zhang, M.; Gao, Y.; Dahn, J. R. Synthesis and electrochemistry of $\text{LiNi}_x\text{Mn}_{2-x}\text{O}_4$. *J. Electrochem. Soc.* **1997**, *144*, 205–213.

(13) Gao, Y.; Dahn, J. R. The high temperature phase diagram of $\text{Li}_{1+x}\text{Mn}_{2-x}\text{O}_4$ and its implications. *J. Electrochem. Soc.* **1996**, *143*, 1783–1788.

(14) Paulsen, J. M.; Dahn, J. R. Phase diagram of Li-Mn-O spinel in air. *Chem. Mater.* **1999**, *11*, 3065–3079.

(15) Zhao, Y.; Yang, Y.; Cao, Y.; Ai, X.; Yang, H.; Xiao, L. Enhanced electrochemical stability of Al-doped LiMn_2O_4 synthesized by a polymer-pyrolysis method. *Electrochim. Acta* **2008**, *54*, 545–550.

(16) Ziolkiewicz, S.; Lemal, M.; Massot, M.; Julien, C. Synthesis, structure, and electrochemistry of $\text{LiMn}_{2-y}\text{Al}_y\text{O}_4$ prepared by a wet-chemistry method. *J. Mater. Chem.* **2001**, *11*, 1837–1842.

(17) Ariyoshi, K.; Iwata, E.; Kuniyoshi, M.; Wakabayashi, H.; Ohzuku, T. Lithium aluminum manganese oxide having spinel-framework structure for long-life lithium-ion batteries. *Electrochim. Solid-State Lett.* **2006**, *9*, A557–A560.